

Large Holocene morphogenic earthquakes along the Albox fault, Betic Cordillera, Spain

E. Masana^{a,*}, R. Pallàs^a, H. Perea^a, M. Ortuño^a, J.J. Martínez-Díaz^b,
E. García-Meléndez^c, P. Santanach^a

^a *Department Geodinàmica i Geofísica, Universitat de Barcelona, Zona Universitaria de Pedralbes, 08028 Barcelona, Spain*

^b *Departamento de Geodinámica, Facultad de Ciencias Geológicas, Universidad Complutense de Madrid, Spain*

^c *Area de Geodinámica Externa, Facultad de Ciencias Ambientales, Universidad de León, Campus de Vegazana s/n, 24071 León, Spain*

Received 18 November 2004; received in revised form 14 April 2005; accepted 18 July 2005

Abstract

The Eastern Betic Shear Zone (EBSZ) in the Betic Cordillera (southern Spain) accommodates part of the Neogene and Quaternary shortening between the Iberian and the African plates. Although the EBSZ is characterised by shallow low to moderate magnitude instrumental seismicity, it seems to be the source of several historical catastrophic events with MSK intensities ranging from VII to X. Despite the fact that it crosses a densely populated area, the seismogenic behaviour of the EBSZ is still poorly understood. The EBSZ is mainly formed by a set of NE–SW-trending left-lateral strike-slip faults, including the Alhama de Murcia and Albox faults. This paper presents a palaeoseismological study of the eastern Albox fault based on surface and trenching observations. This fault ruptures the surface and is probably seismogenic, with short-term slip-rates ranging from 0.01 to 0.4 mm/a. Ground effects of at least two paleoearthquakes were detected: the first one took place not long before 660 years A.D. with an estimated maximum M_w of 6.5 ± 0.1 , whereas the second one occurred between 650 A.D. and the XVIII century. The latter produced only a centimetric offset and was not regarded as characteristic. The elapsed time is, therefore, ca. 660 years. The distribution of the long-term cumulative and the short-term ground effects suggest an eastwards migration of the fault tip.

© 2005 Elsevier Ltd. All rights reserved.

Keywords: Ground effects; Palaeoseismology; Trenching; Albox fault; Trans-Alboran Shear Zone; Betic Cordillera

1. Introduction

A crustal shortening of 4.5–5.6 mm/a is currently being accommodated along the Iberian and African plate boundary (Argus et al., 1989; DeMets et al., 1990, 1994; Kiratzi and Papazachos, 1995; Ponderrelly, 1999; McClusky et al., 2003). The wide distribution of seismicity along this collisional boundary and the absence of fast moving faults in the area suggest a diffuse deformation. In the southeastern Iberian Peninsula the Eastern Betic Shear Zone (EBSZ), formed by NE–SW-trending left-lateral strike-slip faults, has accommodated a large part of the Neogene and Quaternary shortening (Bousquet, 1979; Sanz de Galdeano, 1990).

* Corresponding author. Tel.: +34 93 402 13 72; fax: +34 93 402 13 40.
E-mail address: eulalia.masana@ub.edu (E. Masana).

Despite the low instrumental seismicity, some of these faults display a geomorphological expression, suggesting that they are tectonically active (Montenat, 1977; Bousquet, 1979; Silva et al., 1992, 1993, 2003; Martínez-Díaz and Hernández-Enrile, 1992; Alfaro, 1995; Bell et al., 1997; Martínez-Díaz, 1998; Reicherter and Reiss, 2001; García-Meléndez et al., 2003; Soler et al., 2003; Masana et al., 2004). However, there is little information on the seismogenic nature of the EBSZ. The only palaeoseismological study carried out along this system, including the analysis of four trenches, provided strong evidence of the seismogenic nature of the Lorca-Totana segment of the Alhama de Murcia fault (Martínez-Díaz et al., 2001; Masana et al., 2004) (Fig. 2). This study shows that palaeoseismology can contribute to the characterisation of these faults and, consequently, to a better estimate of the seismic hazard of this densely populated area.

The present paper seeks to characterise the seismogenic nature of the eastern portion of the Albox fault within the EBSZ and to determine its seismotectonic parameters. At this regard, after a geomorphological analysis of the Huércal-Overa area we focused on the eastern prolongation of the Albox fault, which accommodates the overall deformation in this area. We performed a detailed palaeoseismological analysis of four trenches in an attempt to find evidence of the ground effects produced by past earthquakes.

2. Geological setting: from the Transalboran shear zone to the eastern Albox fault

The Betic Cordillera, an ENE–WSW-trending belt, together with the Rif, constitutes an alpine arc-shaped thrust-belt divided into the External and the Internal zones (Fallot, 1948; Andrieux et al., 1971; Fig. 1). The Betics display contemporaneous thrusting in the whole range and extension in the internal parts (Alboran Sea). A stack formed by the Alpujarride, Maláguide and Nevadofilábride units with different metamorphic grades make up the internal zones. Mesozoic to Tertiary rocks form the external zones. A number of Neogene and Quaternary basins are superimposed

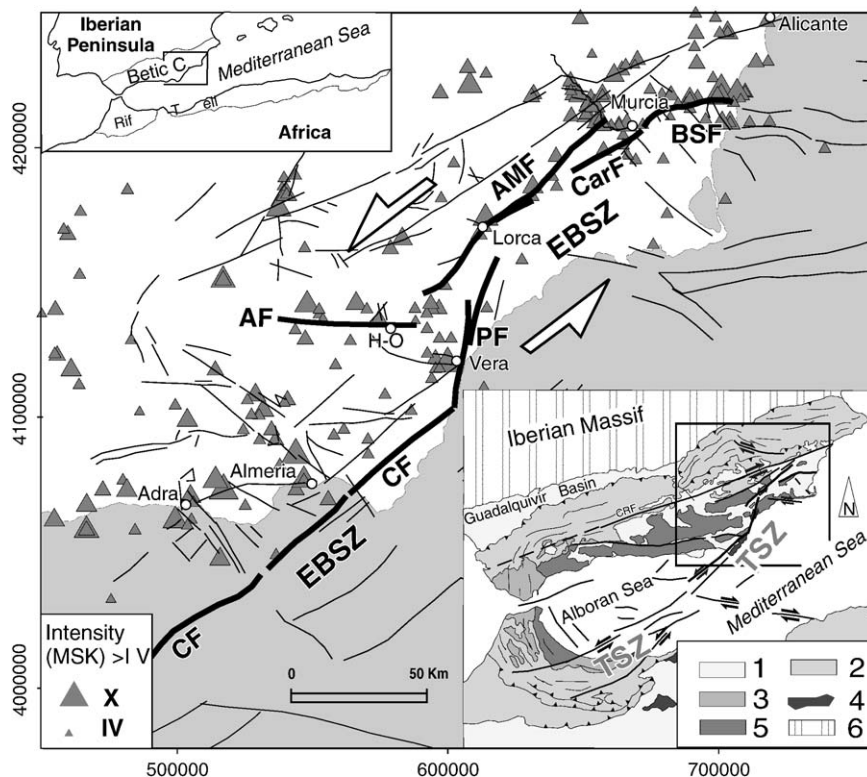


Fig. 1. Map of the Eastern Betic Shear Zone (EBSZ) constituted by—BSF: Bajo Segura fault, CarF: Carrascoy fault, AMF: Alhama de Murcia fault, PF: Palomares fault, CF: Carboneras fault and AF: Albox fault. Triangles indicate epicenters of intensity (MSK) > IV earthquakes for the period 1000–2003 (IGN, 2003). (Lower right) Geological map of the Betic-Rif chain. 1, Neogene and Plio-quaternary; 2, external zones; 3, Flysch nappes; 4, Neogene volcanic rocks; 5, internal zones; 6, Iberian Massif. UTM coordinates in m. TSZ: Trans-Alboran Shear Zone.

onto the previous structure and limited by E–W (e.g. Albox fault) and NE–SW faults (e.g. the Alhama de Murcia fault) (Sanz de Galdeano, 1990).

Present day deformation is driven by NNW–SSE plate convergence (Watts et al., 1993) affecting a wide area (more than 1500 km from the Pyrenees to the Atlas including the Betics and the Rif-Tell). The EBSZ is part of the Trans-Alboran Shear Zone system, which runs from Alacant to the African plate through the Alboran Sea (Larouzière et al., 1987).

2.1. The Eastern Betic Shear Zone. An active structure

The EBSZ is mainly formed by NE–SW-trending left-lateral strike-slip faults (the Bajo-Segura, Carrascoy, Alhama de Murcia, Palomares and Carboneras faults) (Fig. 1).

Seismicity in the EBSZ (Fig. 1) is mainly characterised by shallow low to moderate magnitude earthquakes (Instituto Geográfico Nacional, 2001; Udías et al., 1976; López-Casado et al., 1995). Some historical catastrophic events also occurred with MSK intensities ranging from VII to X, like the Torrevieja earthquake (1829, $I_{MSK} = X$) in the Bajo Segura fault area, the Lorca earthquakes (1579 and 1674, $I_{MSK} = VIII$) along the Alhama de Murcia fault and the Vera (1518, $I_{MSK} = IX-X$; 1863, $I_{MSK} = VII$) and Almeria (1487; 1522, $I_{MSK} = IX$; 1658, $I_{MSK} = VIII$; 1804, $I_{MSK} = IX$) earthquakes in the southern part of the EBSZ (Instituto Geográfico Nacional, 2001).

During the Miocene, a WNW–ESE maximum horizontal compressional axis favoured dextral slip along ENE trending faults (Sanz de Galdeano, 1983, 1990). Since the Tortonian, the horizontal maximum compressional axis has been NNW–SSE and some of the pre-existing NE–SW and SE–NW trending faults have been reactivated as left and right lateral, respectively (Montenat et al., 1987; Mora-Gluckstadt, 1993; Martínez-Díaz, 1998). During this period most of the shortening in the Eastern Betics was accommodated by the EBSZ.

The neotectonics of this shear system has been the object of a number of studies. Intense folding has been described in Quaternary sediments over the reverse south dipping Bajo Segura blind fault (Montenat, 1977; Alfaro, 1995). Extensive geomorphic evidence of recent tectonic activity along the Alhama de Murcia fault is described in detail in Section 2.2. Finally, the Carboneras fault is also considered to have recent activity given its morphological features such as straight mountain fronts, deflected talwegs (bayonets) and offset marine terraces (Bousquet, 1979; Bell et al., 1997; Reicherter and Reiss, 2001; Silva et al., 2003).

2.2. The segmented and seismogenic Alhama de Murcia fault

The Alhama de Murcia fault strikes NE–SW and runs along 100 km from the Huércal-Overa basin to Murcia. Based on the geophysical data, it may also reach the Crevillente fault to the north (Gauyau et al., 1977). It separates the Neogene Guadalentín depression from the Sierra Espuña, La Tercia and Las Estancias ranges (Fig. 2). The neotectonic activity of the Alhama de Murcia fault is well defined by its morphological expression (triangular facets, entrenchment and gradient index anomalies) and by the deformation structures in Quaternary deposits, which provide evidence of left-lateral and local reverse-slip components (Martínez-Díaz and Hernández-Enrile, 1992; Silva et al., 1992, 1993, 2003; Martínez-Díaz, 1998; Martínez-Díaz et al., 2003; Soler et al., 2003). Four segments have been described along this fault based on geometry, fractal signature, deep structure and morphologic features: (1) the segment to the south of Lorca (38 km in length) with scant seismicity and with compressional structures at the southern end where the fault splays out in a horsetail structure to the west; (2) the Lorca-Totana segment (16 km in length), where the maximum concentration of current seismicity is found and where some compressional structures are present due to a slight change in strike; (3) the Totana-Alhama de Murcia segment (17 km in length); (4) the Alhama de Murcia Alcantarilla segment (23 km in length). The last two segments show very little morphological expression and scant seismicity (Silva et al., 1992; Martínez-Díaz and Hernández-Enrile, 1999).

Active dip-slip faulting is usually easier to analyse than strike-slip because it modifies more the surface expression and, therefore, it triggers more surface erosional and depositional processes that could record a palaeoearthquake (McCalpin, 1996). Two sectors where reverse faulting is favoured show up along the Alhama de Murcia fault. The first sector is located in the N060°E Lorca-Totana segment where a palaeoseismological investigation has been carried out (Martínez-Díaz et al., 2001; Masana et al., 2004). These studies have detected ground effects generated by the fault motion and provided strong evidence for the seismogenic nature of the Lorca-Totana segment, indicating a minimum of two (possibly three) Mw 6.5–7 earthquakes during the last 28 ka (named as events N and T). The seismic potential

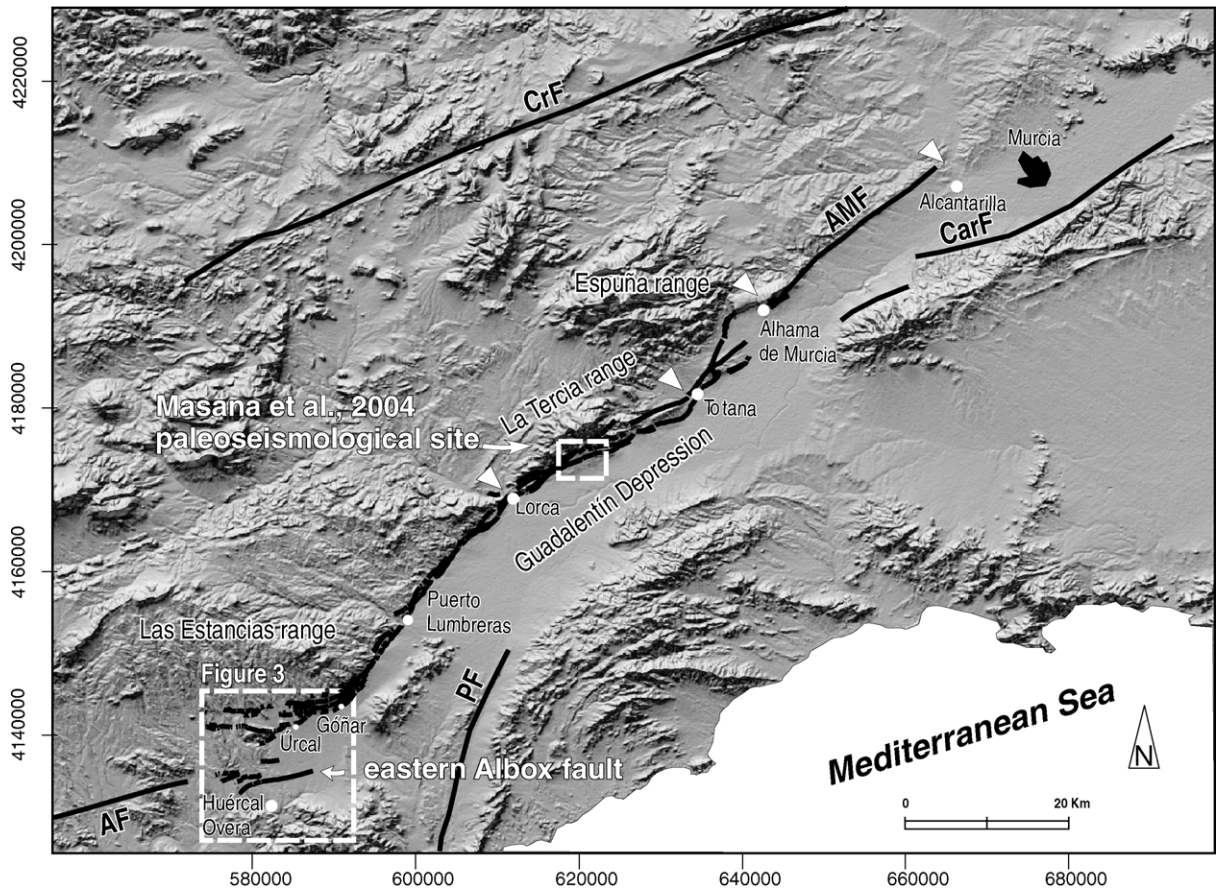


Fig. 2. Shaded relief map of the Alhama de Murcia fault area (illumination from the NW). CrF: Crevillente fault, CarF: Carrascoy fault, AMF: Alhama de Murcia fault, AF: Albox fault. The four segments of the Alhama de Murcia fault are limited by white triangles. The white square shows the Huércal-Overa region and the eastern Albox fault. UTM coordinates in m.

of this segment (considering three events since 28 ka) is characterised by a mean recurrence period of ca. 14 ka, a very short elapsed time (the last event, T, occurred shortly before 1650 A.D.) and a net slip-rate of 0.07–0.6 mm/a (Martínez-Díaz et al., 2001; Masana et al., 2004). The second sector prone to reverse faulting is the southern tip of the Alhama de Murcia fault. South and west of Goñar, the fault splays out into several reverse E–W-striking fault branches forming the Goñar horsetail structure to the west and entering the Huércal-Overa Neogene basin. This is the area investigated in the present paper.

2.3. The Huércal-Overa basin, where the Albox and the Alhama de Murcia faults meet

The Huércal-Overa Neogene basin abuts on the Las Estancias range where Alpujarride rocks crop out. To the south, it is bounded by the Almagro range composed of Alpujarride and locally Maláguide rocks (Fig. 3). Several faults converge eastwards (the Goñar horsetail structure) merging with the NE–SW Alhama de Murcia fault near Goñar. To the west, the soft relief controlled by these reverse faults gradually disappears after some kilometres. The WSW–ENE Albox fault (García-Meléndez, 2000) crosses the Huércal-Overa basin south of the Goñar horsetail structure. This Neogene normal fault has been currently reactivated as a reverse fault probably controlled by the activity along the Alhama de Murcia fault.

The sedimentary fill of the Huércal-Overa basin, which is Neogene in age, begins with an alluvial unit of Serravallian to Tortonian red breccias and conglomerates and it continues with a Tortonian–Messinian unit consisting of sandstone, siltstone, marl and some reefal limestone (Briend, 1981; Mora-Gluckstadt, 1993). Finally, these sequences are unconformably overlain by continental Plio-Quaternary alluvial fans. A series of such fans has been documented in

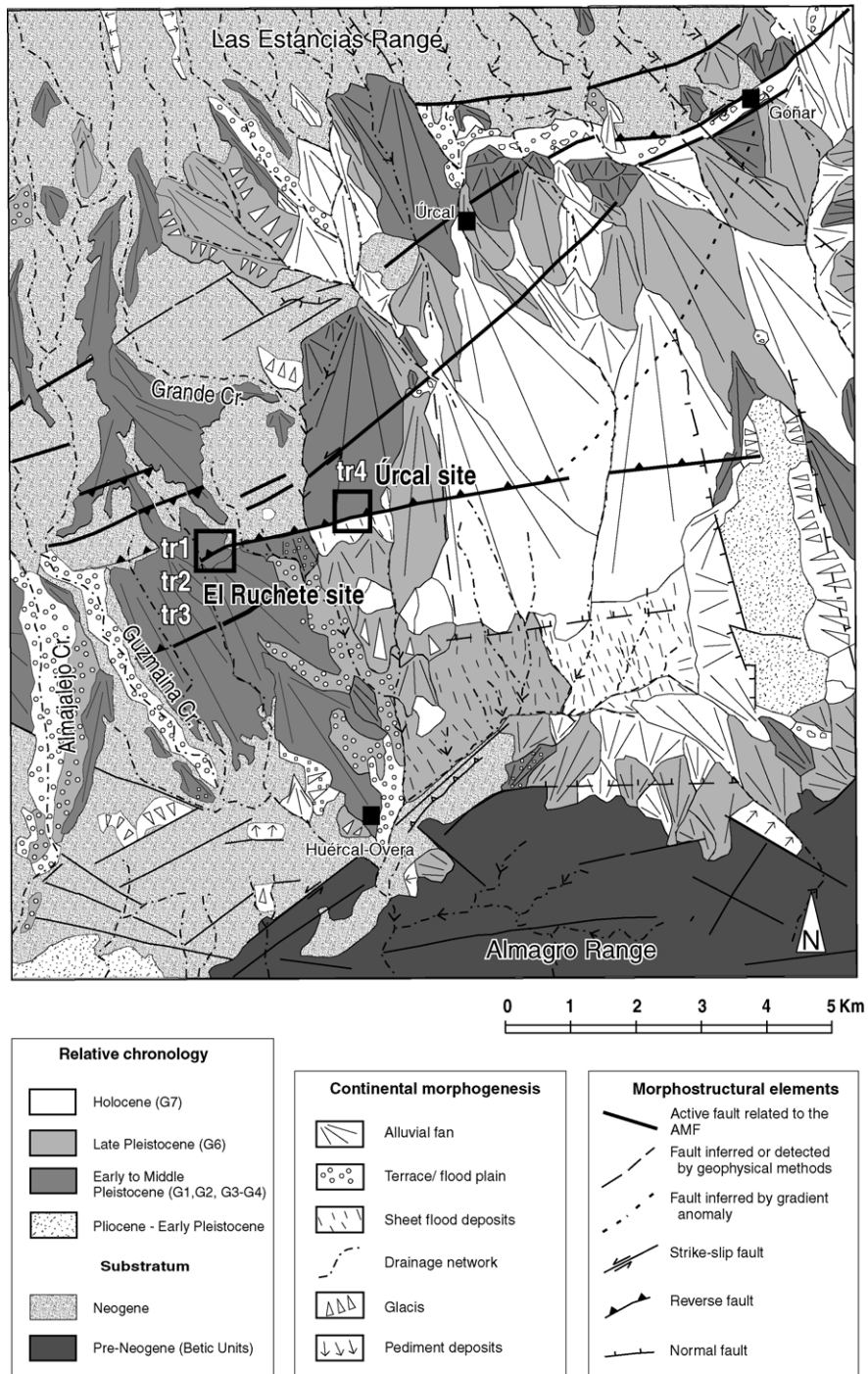


Fig. 3. Geomorphic map of the eastern Huércal-Overa basin, between Las Estancias and Almagro ranges. Location in Fig. 2. Squares in black show the location of the El Ruchete and Úrcal sites along the eastern Albox fault.

the Huércal-Overa basin (García-Meléndez et al., 2003, 2004; Soler et al., 2003), termed G1, G2, G3–G4, G5, G6 and G7 by Soler et al. (2003). In the western part of the Huércal-Overa basin these fans show sequences of entrenchment and aggradation, whereas to the east, which constitutes the subject of the present study, the different fan generations overlap (García-Meléndez, 2000; García-Meléndez et al., 2004). Their relative ages have been estimated by morphologic and

stratigraphic correlation with neighbouring basins (García-Meléndez et al., 2003; Soler et al., 2003): Holocene (G7), Late Pleistocene (G6), Early to Middle Pleistocene (G1, G2, G3–G4).

Sedimentary and structural studies (Briend, 1981; Mora-Gluckstadt, 1993) in the Huércal-Overa basin suggest that the Early Miocene sedimentation was controlled by E–W normal faults. Since the Late Messinian the NE–SW left-lateral strike-slip movement along the Alhama de Murcia fault has strongly influenced the structure (Mora-Gluckstadt, 1993) and the E–W faults have been reactivated as reverse faults along the Goñar horsetail and, during the Quaternary, along the Albox fault (García-Meléndez, 2000). The Quaternary activity within the northern border of the basin has also been documented by sedimentological, geomorphological and structural investigations (Briend, 1981; García-Meléndez et al., 2003, 2004; Soler et al., 2003). Soler et al. (2003) measured the vertical displacement of G2 (140 m) by geometrically reconstructing cross sections, but could not provide good age constraints to estimate a realistic vertical slip-rate.

The Huércal-Overa basin is characterised by moderate to low seismicity. The first recorded earthquake in the area is an $I_{MSK} = IV$ earthquake that occurred in 1756 (Instituto Geográfico Nacional, 2001). The maximum intensity earthquakes recorded are three $I_{MSK} = VI$ events in 1863 and the maximum magnitude event recorded instrumentally is an $M_b = 4.0$, in 1950.

2.4. The eastern Albox fault

Previously described by Briend (1981), Wenzens and Wenzens (1995), García-Meléndez et al. (2003, 2004) and Soler et al. (2003), the eastern WSW–ENE Albox fault crosses the Huércal-Overa basin (Fig. 2). Consecutive creeks located between the eastern tip of the Albox fault and the southern end of the Alhama de Murcia fault show positive anomalies (slope larger than expected) aligned in a NNE–SSW trend. According to Soler et al. (2003), these anomalies indicate that the Alhama de Murcia fault joins the eastern tip of the Albox fault and suggest their current structural link.

These same authors suggest that the eastern Albox fault displays a much higher vertical displacement in cross section than any of the other faults located further to the north in the Huércal-Overa system. This is why we suggest that the eastern Albox fault accommodated most of the N–S shortening during recent times. This fault strongly dips to the north (probably an inherited dip from an earlier Early Miocene normal fault) and shows slickensides indicating an almost pure reverse kinematics (Soler et al., 2003). Thus, it is assumed that the Albox fault represents the overall shortening associated with the left-lateral motion along the Alhama de Murcia fault during Quaternary times.

The fault offsets the surface of several G3–G4 alluvial fans along 4 km and, according to a detailed digital elevation model, it continues for about 5 km further to the east (García-Meléndez et al., 2003). The ground effects of the cumulative fault motion are printed in the offset distribution: offset is larger in the central portion (where the Miocene marls are exhumed in the uplifted block) and it decreases towards the tips. It can only be detected with the digital model of the terrain east of Úrcal. The northern fault block is uplifted, while the fault plane either ruptures the surface or asymmetrically folds it, forming a fault-propagation anticline with a horizontal northern limb and a southern limb strongly dipping to the south. The alluvial fans affected by the fault are separated by unconformities, clearly visible near the fault (G3 and G4 are considered jointly).

3. Methods

This work is the result of: (1) a geomorphological study along the complete Alhama de Murcia fault; (2) a palaeoseismological analysis of the Eastern Albox fault.

The geomorphological study was based on the analysis of aerial photographs (scale 1:33,000 and 1:18,000) followed by fieldwork. A number of faults and ground disruption localities were pre-selected for the palaeoseismological analysis but, after inspection in the field, only the eastern Albox fault was considered adequate with two suitable sites: the El Ruchete and Úrcal sites (Fig. 3).

The palaeoseismological investigation consisted of a detailed near-fault analysis, including the levelling of micro-topographic maps and profiles by a Leica total station 1700. Three trenches were dug at El Ruchete and one at Úrcal (respectively, 37, 10, 18 and 33 m long). A 1-m grid was installed at each wall and a photographic mosaic was printed and used for the logging of trench walls in the field. Dating with AMS Radiocarbon (Gastropoda shells), U/Th (laminar calcrete soils) and TL (in fine grained sediments) provided the age constraints.

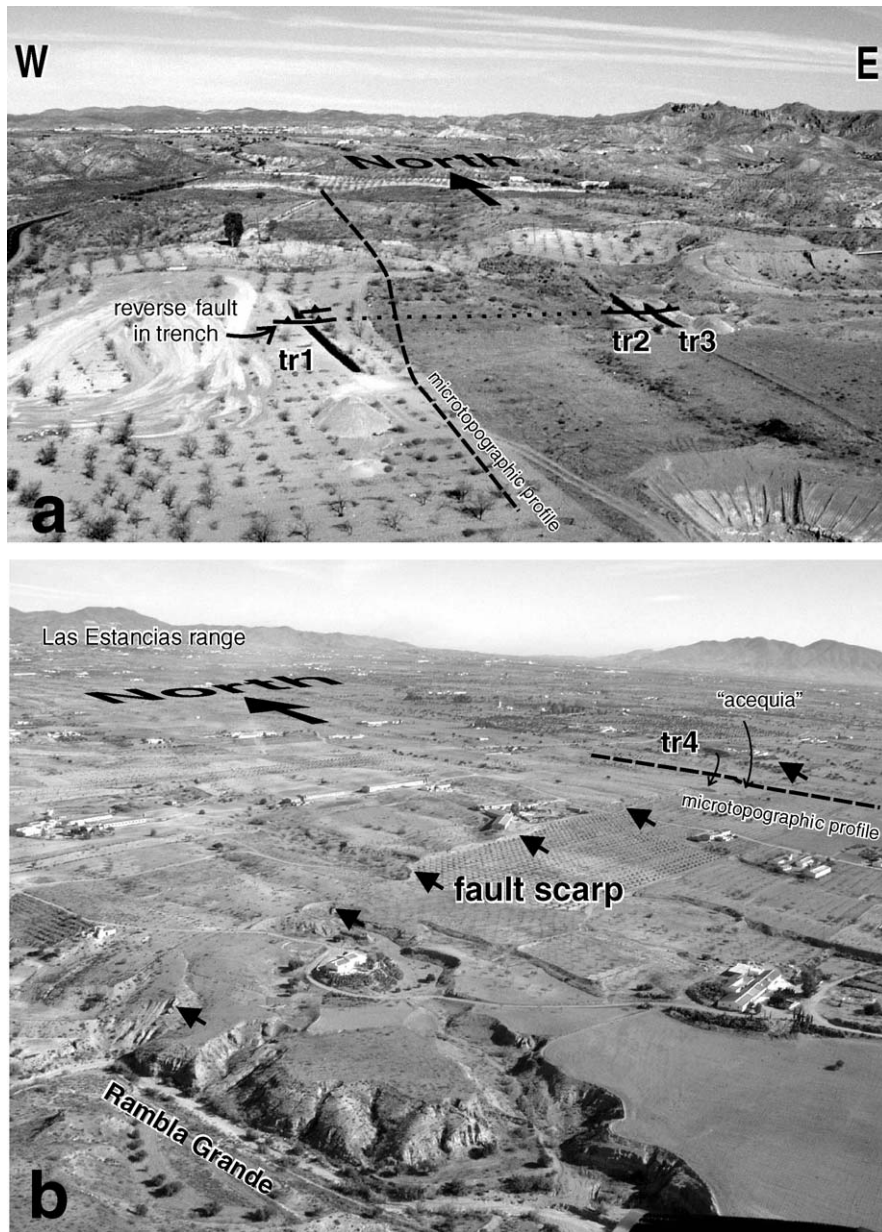


Fig. 4. (a) Aerial oblique photograph of the eastern Albox fault at the El Ruchete site with location of trenches 1, 2 and 3 across the 20 m high fault scarp. (b) Aerial oblique photograph of the eastern Albox fault at the Úrcal site with location of trench 4 across the 5 m high cumulative fault scarp. Black arrows indicate the location of the fault scarp.

4. Results

4.1. The El Ruchete site

This site is located 5 km north of Huércal-Overa some meters east of the Santa María de Nieva road. The microtopographic analysis shows a smooth and 20 m high fault scarp at this site (Figs. 4 and 5). The surface of the G3–G4 alluvial fans is offset and a young reddish local deposit lies at the foot of the scarp. Trench 1 was excavated along a smooth gully and trenches 2 and 3 were cut along a water divide (Fig. 5). Trench 2 revealed structures similar to those in the northern part of trench 3 and is not described here.

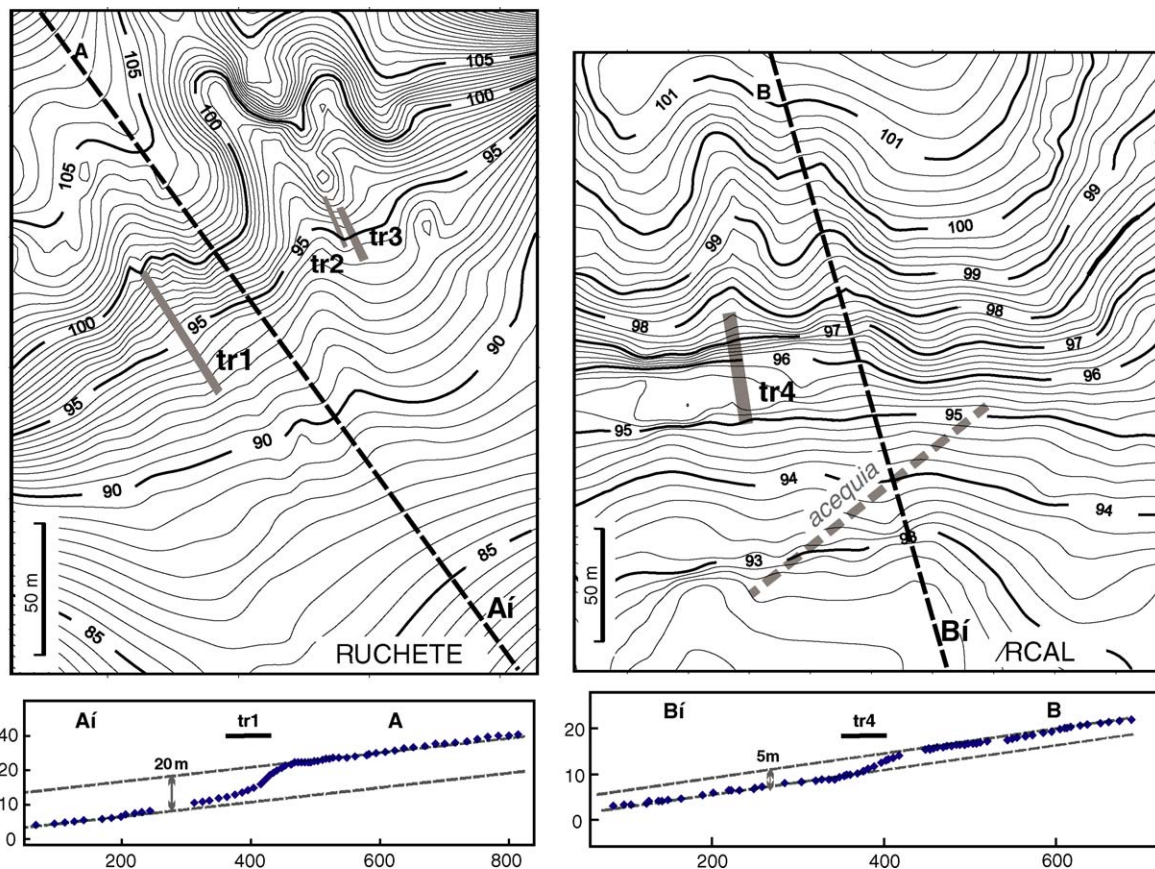


Fig. 5. Microtopographic maps and profiles of the two analysed sites along the eastern Albox fault. Contour lines every 1 m. The location of the palaeoseismological trenches is represented as grey boxes. Topographic profiles are longer than the rectangle included in the map.

4.1.1. Trench 1

Owing to wall collapses, only parts of trench 1 were logged (Fig. 6 shows the northern part of the eastern wall and the southern part of the western wall). The log of the western wall shows the G3–G4 alluvial fan (unit A) composed of loose clast-supported grey gravels and some silty layers dipping southwards. A well-developed calcic soil with laminar facies (unit B) formed at the top of the alluvial fan, overlain by an up to 60 cm thick reddish silty and clayish unit (unit C). These units are covered by loose gravels (units D, E and F), of which only unit E shows some internal structure. The log of the eastern wall shows the northern portion of the trench, which was not visible in the collapsed western wall. The eastern wall shows the G3–G4 alluvial fan sediments (unit A) with the same units observed in the western wall but with some additional local units (M, N and P). Units M and N are located at the footwall of fault F1 and have a wedge shape. Unit M consists of very loose clast-supported gravels, while unit N is composed of loose matrix-supported gravels. Unit P overlies unit N. Unit A₁ corresponds to a 0.5 m thick fault breccia. Fault F1 formed at the base of unit A₁. These breccias are more consolidated with respect to the surrounding units, probably because of their higher permeability.

Evidence of two dislocation events was found in the eastern wall along F1. Units M and N were interpreted as a colluvial wedge generated as a consequence of a dislocation along F1 (event X). The second event (event Y) is inferred from the centimetric dislocation of units M and N along F1, which does not affect unit D.

Some layers in trench 1 were dated as summarised in Table 1. As Gasteropoda shells dated with radiocarbon were in situ and syn-depositional, these samples were considered to be more reliable than the TL should there be discrepancies. Sample Ruc21 (TL) was ruled out given the discrepancy with the radiocarbon results (Ruc1 and Ruc3). Its location within a colluvial wedge suggests a short period of exposure to sunlight and possibly an incomplete bleaching with the result that, in this case, radiocarbon ages are considered to be more reliable. Sample Ruc22 (TL) was also rejected given

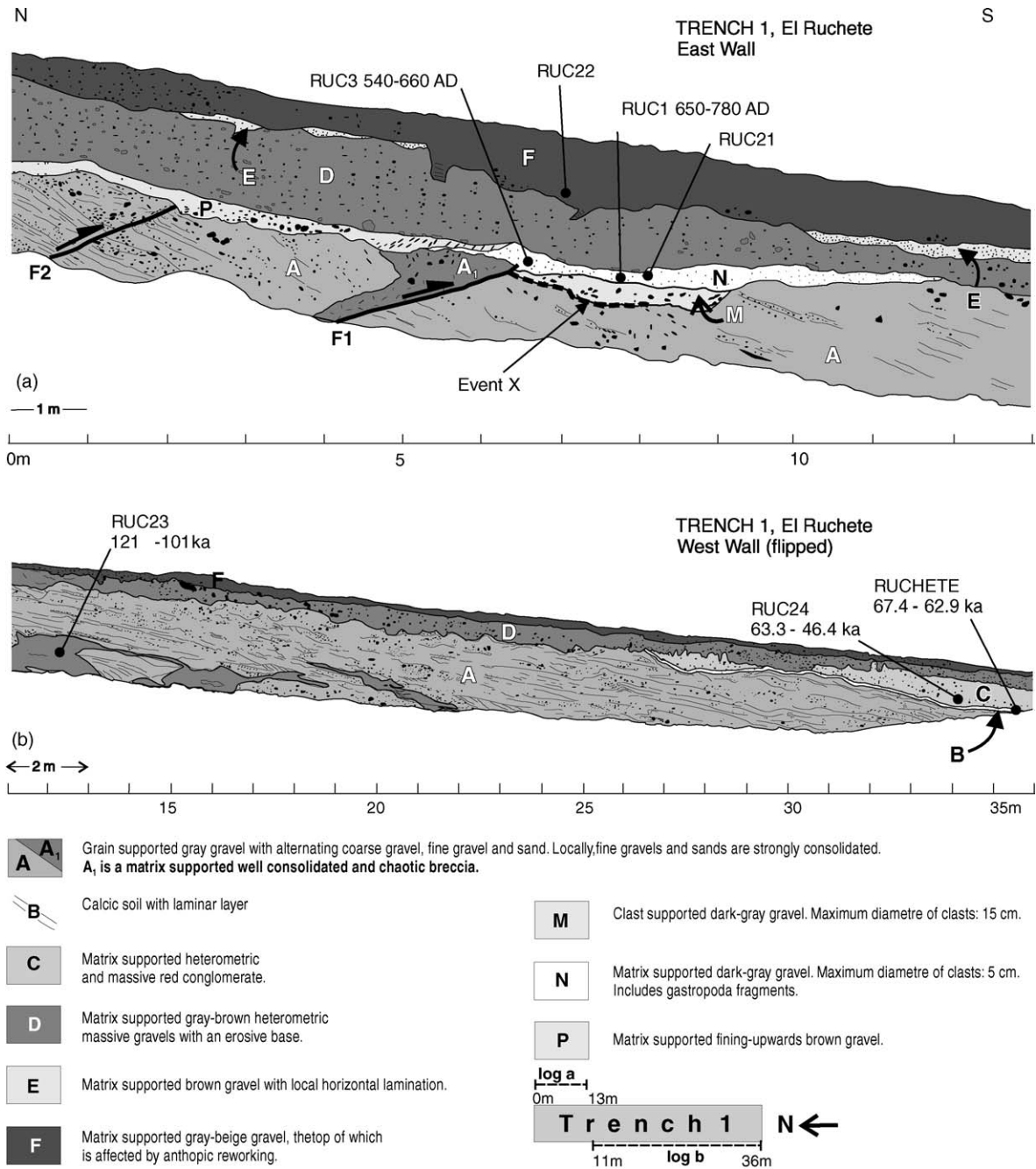


Fig. 6. Log of trench 1: (a) shows the southern part of the western wall; (b) the northern part of the eastern wall. Horizontal and vertical scales are the same. This trench was not logged continuously because of wall collapses. No vertical exaggeration.

that it yielded a much older age than the radiocarbon samples from lower layers. The remaining dates are consistent with one another and with the geological constraints. By correlating with other sedimentary units in neighbouring areas, García-Meléndez et al. (2003) and Soler et al. (2003) assigned a Middle Pleistocene age to the G3–G4 alluvial fans. Radiometric dating suggests a slightly younger age, the top of the fan being bracketed between 121 ka (RUC23) and 63 ka (RUCHETE U/Th).

The age of event X ranges between the ages of units C (younger than 63.3 ka) and N (older than 660 A.D.). Such a long interval is due to the large hiatus registered on top of the G3–G4 alluvial fan and is not uncommon in

Table 1

Numeric dating results from the radiocarbon (^{14}C), uranium/thorium ($^{230}\text{U}/^{232}\text{Th}$) and thermoluminescence (TL) methods

Trench	Sample	Material	C13/C12 (‰)	13C/12C (‰)	14C age BP	Calculated age (2 s interval)
14C dating						
TR1E	RUC1	Gasteropoda shell	-21.0	-7	1310 ± 40	650–780 A.D.
TR1E	RUC3	Gasteropoda shell	-22.6	-3.3	1450 ± 40	540–660 A.D.
Trench	Sample	Material	Th230/Th232	Age U/Th (ka BP)	U/Th age range (ka BP)	
230U/232Th dating						
TR1W	RUCHETE	Laminar calccrete	2.16	65.194 (+2.247/-2.204)	67.4–62.9	
Trench	Sample	Material	Age TL (ka BP)		TL age range (ka BP)	
TL dating						
TR1E	RUC21	Brown silt (N)	8.02 (±0.78)		8.8–7.2	
TR1E	RUC22	Yellowish silt (F)	94 (+21/-14)		115–80	
TR1W	RUC23	Grey-brown silt (A)	121 (+inf/-20)		121–101	
TR1W	RUC24	Red silts (C)	53.9 (+9.4/-7.5)		63.3–46.4	
TR3W	RUC25	Silt and fine sand (A)	104 (+29/-18)		133–86	
TR3W	RUC26	Red silt (C)	68.6 (+12.6/-9.4)		81.2–59.2	
TR3W	RUC27	Red silt (C)	34.2 (+4.1/-3.5)		38.3–30.7	
TR4E	RUC28	White silt (A ₁)	63.2 (+11.6/-8.9)		73.9–53.4	
TR4E	RUC29	Grey silt (O)	11.1 (±0.92)		12.02–10.18	
TR4W	RUC30	Grey sand (A ₂)	56.8 (+6.3/-5)		63.1–51.8	

palaeoseismological studies along slow moving faults. The vertical slip can only be inferred from the thickness of the colluvial wedge (50 cm), which according to Wells and Coppersmith (1994) allows us to estimate a maximum Mw of 6.4 ± 0.1 . However, following McCalpin (1996) the thickness of a colluvial wedge can reach half of the total vertical slip per event and, therefore, a Mw 6.5 ± 0.2 event cannot be ruled out. The age of event Y is only half-bracketed because no samples suitable for dating were available in units younger than unit N. Therefore, event Y occurred after 650 A.D. and defines a very short elapsed time.

4.1.2. Trench 3

Despite being only less than 200 m apart from trench 1, trench 3 (Fig. 7) shows a different deformation pattern. Both walls show a highly deformed G3–G4 fan unit (unit A) with a calcic soil on top (unit B) overthrusting reddish matrix-supported clays and silts (unit C) along a wide deformation zone between faults F1 and F2 (Fig. 7). In the hangingwall, unit A layers are overturned and form the southern limb of an anticline which recovers the normal gentle dip of the fan some tens of metres to the north (visible at trench 2 and natural outcrops). Units A to C are covered by sheet-like sedimentary units (E, F and G), which are attributed to the current soil and to human activity (Fig. 7). The large hiatus represented by the base of these thin units is evidenced by the large amount of deformation in units A, B and C, and the lack of deformation in the younger ones. The large amount of erosion in the hangingwall is probably linked to the tectonic uplift of this block. The units observed in this trench are easily comparable with those in trench 1 owing to their facies (the same letters were used to describe them). Moreover, the ages obtained at this trench (TL and radiocarbon) are consistent with those at trench 1.

Faults F1 and F2 at trench 3 provide evidence of recent surface rupture. In contact with F2, unit A₂ corresponds to consolidated gravels showing a lower degree of internal organisation than the surrounding units. This unit is suggested (with weak evidence) to be the collapsed part of a reverse fault scarp generated by F2. Such an event would have taken place after 133 ka (RUC25) with a minimum offset of ca. 1 m (length of the base of unit A₂). Along F1, a minimum value for the reverse slip-rate of 0.03 mm/a is obtained based on the minimum offset (2 m) of the calcic soil (and part of unit C) clearly visible on the eastern wall, together with its age (maximum age of the calcic soil of 67 ka, TR1W, RUCHETE). This is a minimum value because: (1) it only takes into account one of the two faults documenting recent surface rupture (F2 probably generated more than 1 m of additional displacement); (2) it considers the age of the calcic soil although the fault affects the base of unit C (similar results were obtained by using RUC26 whereas 0.05 mm/a was obtained by using RUC27 although the position of this sample is not clearly

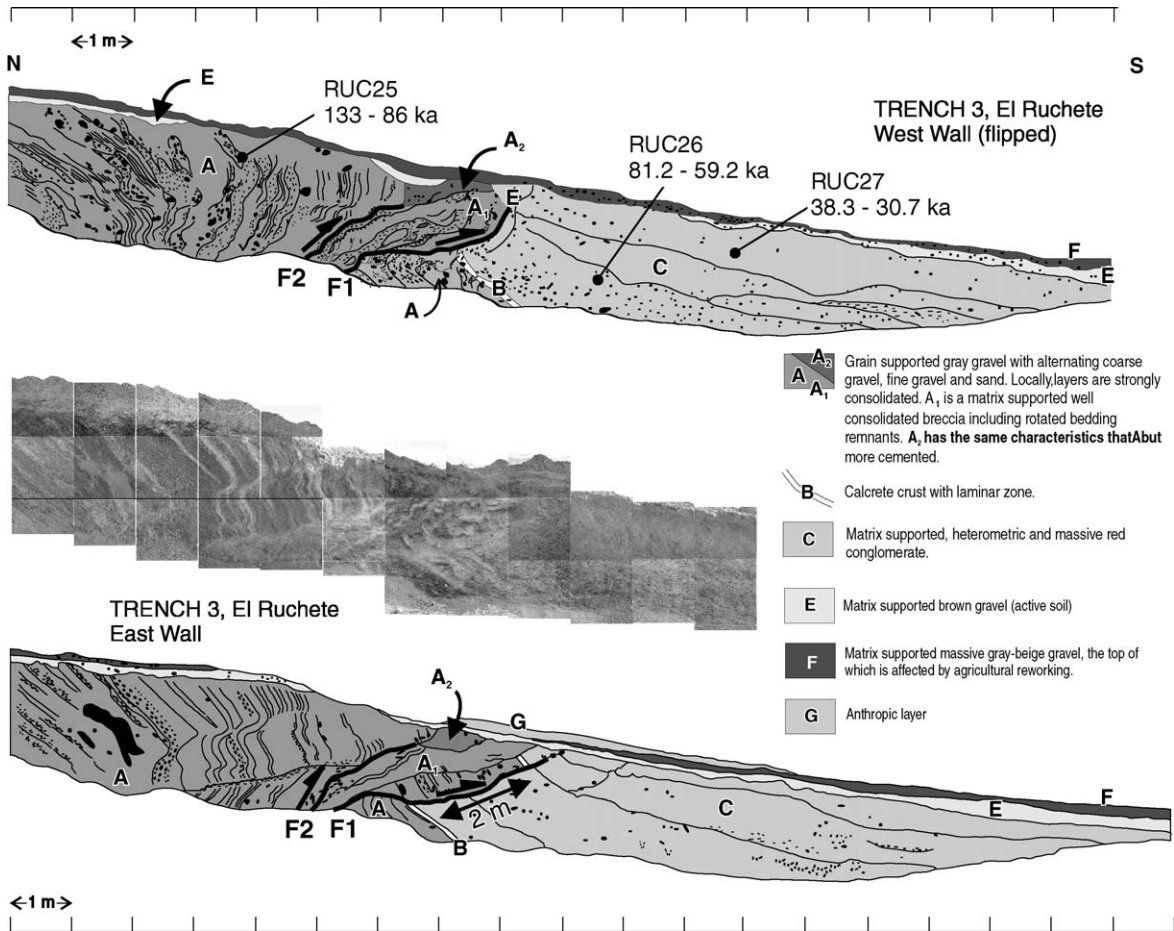


Fig. 7. Log of trench 3 and composition of photographs of part of the eastern wall. Horizontal and vertical scales are the same.

affected by the fault and thus the value was considered as uncertain); (3) because only the oldest part of the age bracket was used.

4.2. The Úrcal site

The site is located midway between Huércal-Overa and Úrcal, 200 m west of the local road. The cumulative morphological fault scarp is only 5 m high according to the microtopographic levelled profiles (Fig. 5). This vertical displacement is also observed from aerial photograph across the G3–G4 alluvial fans despite the intense agricultural activity in the area. West of this location the vertical offset was also detected by digital elevation model treatment (García-Meléndez et al., 2003). Trench 4 was excavated in a very gentle gully to the northwest of an abandoned irrigation channel (*acequia*) as shown in Figs. 4 and 5.

4.2.1. Trench 4

This trench (Fig. 8) shows the G3–G4 alluvial fan (unit A) gently dipping towards the south. G3–G4 alluvial fans are composed of loose gravels with sands and interlayered silts. This trench shows a 0.5 m thick silty layer located in the upper part of the sequence (unit A₁) followed by sub-horizontal gravels with an erosive base located in the southern part of the trench (unit A₂). A reddish loose conglomerate unit (unit O) unconformably covers the alluvial fan sediments. Finally, unit Q, a reddish brown soil eroded by the anthropogenically modified unit F, displays an irregular distribution over the sequence. According to the available age constraints and the geomorphological interpretation, unit A at trench 4 correlates with unit A at the El Ruchete site. Given the radiometric ages obtained on top of the G3–G4

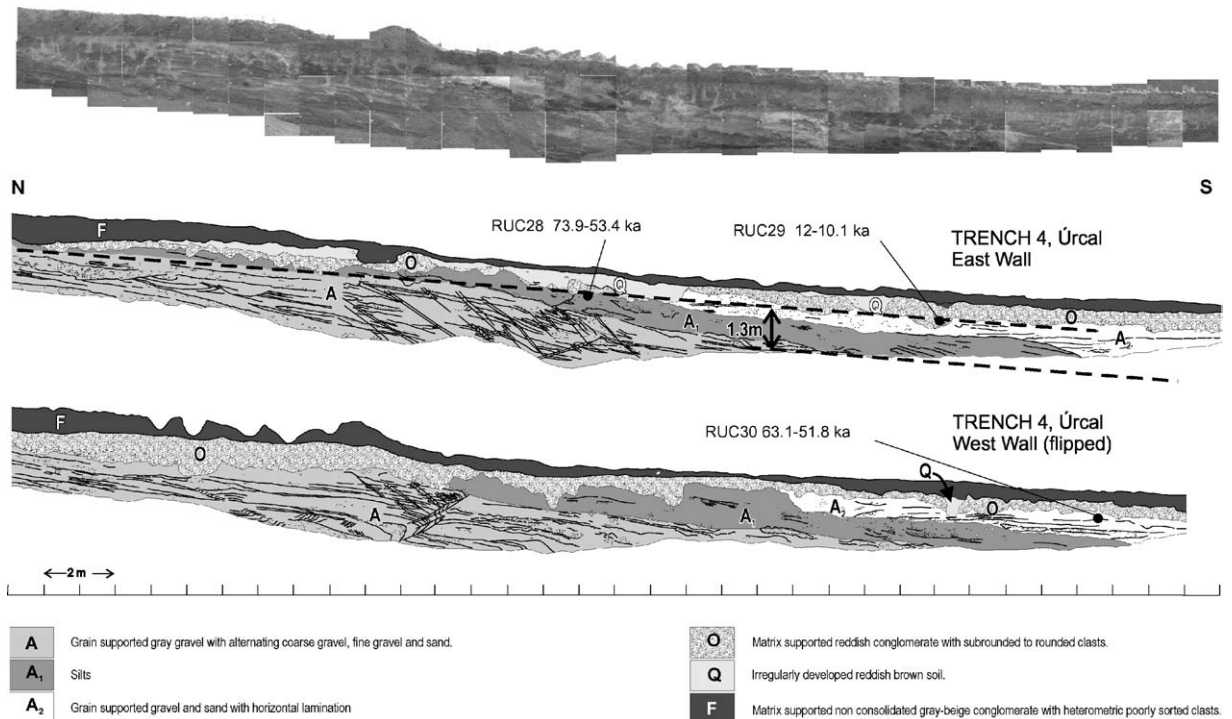


Fig. 8. Log of trench 4 and photograph composition of the eastern wall. Horizontal and vertical scales are the same.

alluvial fan (Table 1, Ruc23 in tr1W, Ruc25 in tr3W, Ruc28 in tr4E and Ruc30 in tr4W), this fan generation ended during the Late Pleistocene.

Unit A is clearly deformed in the zone of the topographic offset. Both western and eastern walls display southwards dipping kink bands that accommodate the deformation of a south-vergent fold that is clearly seen in the western wall. Kink folds do not affect the units overlying unit A. Conversely, unit A₁ is deformed by a gentle fold and generates a minimum of 1.3 m vertical displacement at the trench (possibly larger given that, in the southern part of the trench, this layer does not recover the original slope shown in the northern part). In contrast, A₂ is not obviously affected by the deformation: it horizontally onlaps unit A₁ with an erosive base. A minimum value of differential uplift-rate of ca. 0.02 mm/a is obtained by considering an age of 73.9–53.4 ka (Ruc28) on top of unit A₁. Assuming a 30 dipping fault (dip of the kink bands) the minimum slip-rate is 0.04 mm/a.

5. Discussion

5.1. Implications for the seismogenic nature of the eastern Albox fault

Late Holocene morphogenic activity (sensu Caputo, 1993) along the eastern Albox fault was evidenced at trench 1 where sediments of this age (units M and N) are cut by the fault, while all the trenches show evidence of surface rupture events affecting the top of G3–G4 alluvial fans (Late Pleistocene). Trench 4 shows a superficial flexure coinciding with near surface reverse kink bands. The eastern Albox fault, therefore, can be described as a fault capable of generating ground effects. Evidence of the seismic behaviour of this fault is suggested by the presence of a colluvial wedge at trench 1.

5.2. Slip-rates

Although the displacement of a fault normally decreases towards the tips the short-term differential uplift-rate estimated at El Ruchete site (a minimum of 0.01–0.02 mm/a according to the dip of the faults and the 0.03 slip-rate)

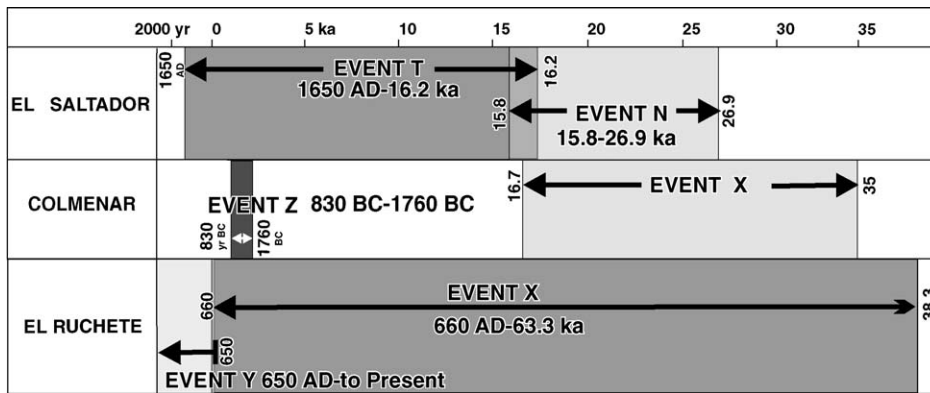


Fig. 9. Synthesis of the palaeoearthquakes detected in the Huércal-Overa (El Ruchete site) and in the Lorca-Totana segments (El Saltador and Colmenar sites).

is slightly lower but similar to that obtained at the Úrcal site (0.02 mm/a), which is located at the eastern tip. These uplift-rates contrast with the long-term cumulative displacement observed along the fault scarp, which is larger at El Ruchete (20 m of topographical offset) than at Úrcal (5 m). This suggests a change in the slip distribution along the fault over time: in the past the vertical offset was larger at El Ruchete than at Úrcal whereas in recent times it is similar on both sites. An eastwards migration of the fault tip can account for this distribution of slip.

The eastern Albox fault is the southernmost expression of the motion along the Alhama de Murcia fault. According to the dip-slip slickensides observed along the trace of the eastern Albox fault (mainly between the two sites investigated in the present paper), the strike-slip component is negligible (Soler et al., 2003). Therefore, the N–S shortening in the eastern Albox fault should be comparable to that along the rest of the Alhama de Murcia fault. The uplift of Las Estancias Range (Fig. 2) would have been controlled by the oblique-slip kinematics along the Alhama de Murcia fault on its southeastern front and by the reverse slip along the Albox fault on its southern front. The inferred reverse 0.03 mm/a slip-rate obtained for the eastern Albox fault corresponds to 0.01–0.02 mm/a of N–S shortening-rate using a fault dip of 60° (measured in creeks such as Grande and Guzmaina, where relatively deep portions of the fault crop out) and 30° (measured at the trenches), respectively. Along the N060° trending Lorca-Totana segment of the Alhama de Murcia fault the strike-slip component of the total slip proposed by Masana et al. (2004) is 0.06–0.53 mm/a, which corresponds to a N–S shortening-rate of 0.03–0.26 mm/a. Therefore the N–S shortening-rate accommodated by the Alhama de Murcia fault may be ten times larger than that observed along the Albox fault. The relative position (Lorca-Totana in the central part and Albox fault at the southern tip) with respect to the central part of the fault where the maximum slip is expected can account for part of this discrepancy. However other considerations may be taken into account: (a) the reverse slip-rate at trench 3 is probably underestimated; (b) the E–W faults and folds in the Goñar horsetail structure can also accommodate part of the strain.

5.3. Seismotectonic parameters

Two palaeoearthquakes were detected along the eastern Albox fault (Fig. 9). The first one, event X, occurred between 38.3 ka and 660 A.D. and generated a 50 cm thick colluvial wedge. By applying the empirical relationships proposed by Wells and Coppersmith (1994) a minimum M_w of 6.4 ± 0.1 can be estimated, although a M_w of 6.5 ± 0.2 cannot be ruled out because the fault offset is usually twice the thickness of the colluvial wedge. Despite the age uncertainty, event X probably took place close to the upper limit of the time window because colluvial wedges develop shortly after the generation of its associated scarp. The second palaeoearthquake (event Y) occurred after 650 A.D. and generated a centimetric offset. Such a small offset may not correspond to a characteristic earthquake. Accordingly, the elapsed time is calculated from event X, i.e. close to ca. 1340 years. Therefore, the elapsed time along this fault is very short. No catastrophic earthquake is recorded in the historical and instrumental seismicity catalogue of the Huercal-Overa area. Therefore, events X and Y may have occurred before the XVIII century, the date of the oldest records in the catalogue.

Event X of the eastern Albox fault could be correlative with events Z and T of the Lorca-Totana segment (Masana et al., 2004) (Fig. 9). Event Y can only be correlated with event T. These possible correlations could be used to suggest

that earthquakes in the area may rupture across segment boundaries. If this could be confirmed, it would be relevant to seismic hazard analysis.

6. Conclusions

The eastern Albox fault is able to generate ground effects and is probably seismogenic. This is the first sign of a seismogenic fault along the EBSZ apart from the ground effects analysed in the Lorca-Totana segment (Alhama de Murcia fault).

The differential uplift-rate obtained at the El Ruchete site (0.01–0.02 mm/a) is similar to or even lower than that at Úrcal (0.02–0.04 mm/a). By contrast, the cumulative displacement is four times larger at El Ruchete. This suggests a change in the distribution of the slip over time. An eastwards migration of the fault tip can account for this distribution of slip.

The N–S shortening-rate deduced for the eastern Albox fault corresponds to the lower limit of published values for the Lorca-Totana segment (Alhama de Murcia fault). This may in part be attributed to the fact that the measurements in Lorca-Totana are in the central sector of the Alhama de Murcia where maximum values are expected. However this explanation does not account for the whole difference. It may be suggested that, although the eastern Albox fault accommodates most of the shortening generated along the Alhama de Murcia fault, folds or minor faults forming the Goñar horsetail structure could also contribute to the deformation.

This palaeoseismic study shows that the eastern Albox fault generated at least two morphogenic earthquakes. Event X occurred not long before 660 A.D. and had a maximum M_w of 6.5 ± 0.1 (considering 1 m of vertical offset). Event Y, of smaller magnitude, occurred after 650 A.D. and, probably, before the XVIII century. The elapsed time is ca. 1340 years.

Acknowledgements

This study was supported by the European SAFE project ENGV-CT-2000-00023. The study would have not been possible without the field assistance of P. Casanovas, V. Clemente, E. Costa, E. Comas, M. Contreras and J. Rabaneda. We also wish to thank the owners of the land where the trenches were dug for permitting access and for providing help. Quaternary TL Surveys (<http://www.users.globalnet.co.uk/~qtls/>) performed TL dating. We are indebted to Dr R. Julià, who carried out U/Th dating at the Institut Jaume Almera de Ciències de la Terra (CSIC) in Barcelona. We are grateful to S. Pavlides, K. Verbeek and R. Caputo for their constructive comments of the manuscript.

References

- Alfaro, P., 1995. Neotectónica en la Cuenca del Bajo Segura (Cordillera Bética oriental). PhD Thesis. Universitat d'Alacant, 215 pp.
- Andrieux, J., Fontboté, J.M., Mattauer, M., 1971. Sur un modèle explicatif de l'Arc de Gibraltar. *Earth Planet. Sci. Lett.* 12, 191–198.
- Argus, D.F., Gordon, R.G., DeMets, Ch., Stein, S., 1989. Closure of the Africa–Eurasia–North America plate motion circuit and tectonics of the Gloria Fault. *J. Geophys. Res.* 94, 5585–5602.
- Bell, J.W., Amelung, F., King, G.C.P., 1997. Preliminary late Quaternary slip history of the Carboneras Fault, southeastern Spain. *J. Geodyn.* 24, 51–66.
- Bousquet, J.C., 1979. Quaternary strike-slip faults in southeastern Spain. *Tectonophysics*, 277–286.
- Briend, M., 1981. Evolution morpho-tectonique du bassin neogene de Huércal Overa (Cordilleres Bétiques orientales-Espagne). *Documents et travaux, IGAL* 4, 208 pp.
- Caputo, R., 1993. Morphogenic earthquakes: a proposition. *Bull. INQUA-Neotectonic Comm.* 16, 24 (Stockholm).
- DeMets, Ch., Gordon, R.G., Argus, D.F., Stein, S., 1990. Current plate motions. *Geophys. J. Int.* 101, 425–478.
- DeMets, Ch., Gordon, R.G., Argus, D.F., Stein, S., 1994. Effect of recent revisions to the geomagnetic reversal time scale on estimate of current late motions. *Geophys. Res. Lett.* 21, 2191–2194.
- Fallot, P., 1948. Les Cordillères Bétiques. *Estudios Geológicos* 4, 259–279.
- García-Meléndez, E., 2000. Geomorfología y Neotectónica del Cuaternario de la cuenca de Huércal-Overa y corredor del Almanzora. Análisis y Cartografía mediante Teledetección y SIG. Unpublished PhD Thesis. Universidad de Salamanca, 528 pp.
- García-Meléndez, E., Goy, J.L., Zazo, C., 2003. Neotectónica and Plio-Quaternary landscape development within the eastern Huércal-Overa Basin (Betic Cordilleras, southeastern Spain). *Geomorphology* 50, 111–133.
- García-Meléndez, E., Goy, J.L., Zazo, C., 2004. Quaternary tectonic activity in the Huércal-Overa Basin (Almería Southeast Spain): deformations associated with the Albox fault. *Geogaceta* 36, 63–66.

- Gauyau, F., Bayer, R., Bousquet, J.C., Lachaud, J.C., Lesquer, A., Montenat, C., 1977. Le prolongement de l'accident d'Alhama de Murcia entre Murcia et Alicante (Espagne Résultats d'une étude géophysiqueméridionale). *Bull. Soc. Géol. France, Série 7* 19, 623–629.
- Instituto Geográfico Nacional (IGN), 2001. Catálogo Sísmico Nacional hasta el 2001. Publicaciones del Instituto Geográfico Nacional.
- Kiratzis, A., Papazachos, C.B., 1995. Active crustal deformation from the Azores triple junction to the Middle East. *Tectonophysics* 243, 1–24.
- Larouzière, F., Montenat, C.H., Ott D'Esteveou, Ph., Gribeaud, P., 1987. Évolution simultanée de bassins néogènes en compression et en extension dans un couloir de décrochement: Inohar et Mazarrón (Sud-Est de l'Espagne). *Bull. Centr. Rech. Explor. Prod. Elf-Aquit.* 11, 23–38.
- López-Casado, C., Sanz de Galdeano, C., Delgado, J., Peinado, M.A., 1995. The b parameter in the Betic Cordillera, Rif and nearby sectors. Relations with the tectonics of the region. *Tectonophysics* 248, 277–292.
- Martínez-Díaz, J.J., 1998. Neotectónica y tectónica activa del sector Centro-occidental de la región de Murcia y sur de Almería (Cordillera Bética-España). PhD Thesis, p. 466.
- Martínez-Díaz, J.J., Hernández-Enrile, J.L., 1992. Tectónica reciente y rasgos sismotectónicos en el sector Lorca-Totana de la falla de Alhama de Murcia. *Estudios Geológicos* 48, 153–162.
- Martínez-Díaz, J.J., Hernández-Enrile, J.L., 1999. Segmentación tectónica de la falla de Alhama de Murcia y actividad palaeosísmica asociada. Contribución a la determinación de la peligrosidad sísmica en la región de Murcia. 1er Congreso Nacional de Ingeniería Sísmica, 75–87.
- Martínez-Díaz, J.J., Masana, E., Hernández-Enrile, J.L., Santanach, P., 2001. Evidence for coseismic events of recurrent prehistoric deformation along the Alhama de Murcia fault, southeastern Spain. *Acta Geológica Hispánica* 36, 315–327.
- Martínez-Díaz, J.J., Masana, E., Hernández-Enrile, J.L., Santanach, P., 2003. Effects of repeated palaeoearthquakes on the Alhama de Murcia Fault (Betic Cordillera, Spain) on the Quaternary evolution of an alluvial fan system. *Ann. Geophys.* 46 (5), 775–792.
- Masana, E., Martínez-Díaz, J.J., Hernández-Enrile, J.L., Santanach, P., 2004. The Alhama de Murcia fault (SE Spain), a seismogenic fault in a diffuse plate boundary. Seismotectonic implications for the Ibero-Magrebien region. *J. Geophys. Res.* 109, 1–17.
- McCalpin, J., 1996. *Paleoseismology*. Academic Press, San Diego, 588 pp.
- McClusky, S.R., Reilinger, S., Mahmoud, D., Ben Sari, Tealeb, A., 2003. GPS constraints on Africa (Nubia) and Arabia plate motions. *Geophys. J. Int.* 155, 126–138.
- Montenat, C., 1977. Les bassins néogènes du levant d'Alicante et de Murcia (Cordillères Bétiques Orientales, Espagne), vol. 79. *Doc. Lab. Géol. Fac. Sci. Lyon*, 345 pp.
- Montenat, C., Ott d'Esteveou, P., Masse, P., 1987. Tectonic sedimentary characters of the Betic Neogene basins evolving in a crustal transcurrent shear zone (SE Spain). *Bull. Centr. Rech. Expl., Prod. Elf Aquitaine* 11, 1–22.
- Mora-Gluckstadt, M., 1993. Tectonica and sedimentary analysis of the Huércal-Overa region, Southeast Spain, Betic Cordillera. PhD Thesis. Oxford University, 232 pp.
- Ponderrelly, A., 1999. Patterns of the seismic deformation in the Western Mediterranean. *Ann. Geofis.* 42, 57–70.
- Reicherter, K., Reiss, S., 2001. The Carboneras Fault zone (southeastern Spain) revisited with Ground Penetrating Radar: Quaternary structural styles from high-resolution images. *Neth. J. Geosci./Geologie en Mijnbouw* 80, 129–138.
- Sanz de Galdeano, C., 1983. Los accidentes y fracturas principales de las Cordilleras Béticas. *Estudios Geol.* 39, 157–165.
- Sanz de Galdeano, C., 1990. Geologic evolution of the Betic Cordilleras in the Western Mediterranean, Miocene to the present. *Tectonophysics* 172, 107–119.
- Silva, P.G., Goy, J.L., Zazo, C., 1992. Structural and geometrical features of the Lorca-Alhama strike-slip fault. *Geogaceta* 12, 7–11.
- Silva, P.G., Goy, J.L., Somoza, L., Zazo, C., Bardají, T., 1993. Landscape response to strike-slip faulting linked to collisional settings: Quaternary tectonics and basin formation in the Eastern Betics, southeast Spain. *Tectonophysics* 224, 289–303.
- Silva, P.G., Goy, J.L., Zazo, C., Bardají, T., 2003. Fault-generated mountain fronts in southeast Spain: geomorphologic assessment of tectonic and seismic activity. *Geomorphology* 50, 203–225.
- Soler, R., Masana, E., Santanach, P., 2003. Evidencias geomorfológicas y estructurales del levantamiento tectónico reciente en la terminación sudoccidental de la falla de Alhama de Murcia (Cordillera Bética Oriental). *Revista de la Sociedad Geológica de España* 16 (3/4), 123–133.
- Udías, A., López-Arroyo, A., Mézcua, J., 1976. Seismotectonics of the Azores-Alboran region. *Tectonophysics* 31, 259–289.
- Watts, A.B., Platt, J.P., Buhl, P., 1993. Tectonic evolution of the Alboran Sea basin. *Basin Res.* 5, 153–177.
- Wells, D.L., Coppersmith, K.J., 1994. New empirical relationships among magnitude, rupture length, rupture area and surface displacement. *Bull. Seismol. Soc. A* 84, 974–1002.
- Wenzens, E., Wenzens, G., 1995. The influence of Quaternary tectonics on river capture and drainage patterns in the Huércal-Overa basin, southeastern Spain. In: Lewin, J., Macklin, M.G., Woodward, J.C. (Eds.), *Mediterranean Quaternary River Environments*. Balkema, Rotterdam, pp. 55–63.